

# Gap resonance analyzed by a domain decomposition method

Trygve Kristiansen and Odd M. Faltinsen

## Introduction

Gap resonance problems is a relevant problem in practice within marine activity and have been addressed in recent years both by industry (Bunnik et al. (2009)) and in more academic works (McIver (2005), Kristiansen and Faltinsen (2009), Molin et al. (2009), Lu et al. (2010)). Examples are ship-by-ship operations, moonpools and LNG carriers alongside terminals. Marine engineers typically meet problems when trying to analyze this theoretically/numerically, in particular when the gap becomes small relative to the body dimensions. This is so since traditional panel methods then greatly overestimate the fluid and body motions around the gap resonance frequencies. The reason is that linear damping from radiated waves is small compared to the damping provided by flow separation e.g. at bilge keels.

It is therefore of interest to develop a method that may be used in an engineering approach that takes flow separation into account. The method should be fast and easy to use. It should also be based on physics.

This has been the goal of the present work. We are at the moment developing a time-domain numerical wavetank based on domain-decomposition. The main part of the wavetank has linearized potential flow, but we incorporate the effect of flow separation using a Naviér-Stokes solver (CFD) in a submerged domain around the body. It is important to note that the CFD-domain is submerged, which means that there is no CFD in the free surface zone. This leads to a cpu-efficient and accurate method as will be exemplified by a moonpool study where we compare with model tests.

The present domain decomposition method is inspired by the study in Kristiansen and Faltinsen (2008); gap resonance problems are well modelled by linear theory, as long as the effect of flow separation is included.

## Theory

Consider a closed two-dimensional wavetank filled with an incompressible fluid as in Figure 1. We assume that in most of the wavetank the fluid is inviscid, but viscous near the ship bilges. The governing equations are the Bernoulli equation in the inviscid domain and the Naviér-Stokes equations in the viscous domain,

$$\frac{\partial \varphi}{\partial t} + 0.5 \nabla \varphi \cdot \nabla \varphi = -\frac{1}{\rho} p - gz, \quad (1)$$

$$\frac{\partial \mathbf{u}}{\partial t} + \mathbf{u} \cdot \nabla \mathbf{u} = -\frac{1}{\rho} \nabla p - g \hat{\mathbf{k}} + \nu \nabla^2 \mathbf{u}, \quad (2)$$

along with the requirement of continuity of mass,

$$\nabla^2 \varphi = 0, \quad (3)$$

$$\nabla \cdot \mathbf{u} = 0. \quad (4)$$

Here,  $\mathbf{u} = (u, w)$  is the fluid velocity and  $\varphi$  is the velocity potential.

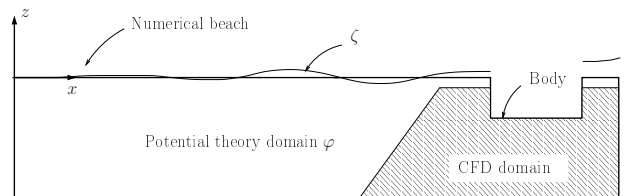


Figure 1: Sketch of numerical wavetank. The domain is fixed and denoted  $\Omega_0$ .

We require that (a) the normal velocity and (b) the pressure is continuous along the boundary that separates the two domains.

We further assume that the fluid flow everywhere away from sharp corners is well described by linear theory, so we neglect the nonlinear term in (1). We introduce the acceleration potential  $\psi = \frac{\partial \varphi}{\partial t}$  which also satisfies the Laplace equation. In the inviscid domain we then have the free-surface problem described by

$$\begin{aligned} \nabla^2 \psi &= 0 && \text{in } \Omega_0, \\ \frac{\partial \varphi}{\partial t} &= \psi && \text{in } \Omega_0, \\ \frac{\partial \zeta}{\partial t} &= \frac{\partial \varphi}{\partial z} && \text{on } z = 0, \\ \psi &= -g\zeta && \text{on } z = 0, \end{aligned} \quad (5)$$

where  $\zeta(x, t)$  is the free surface elevation. For convenience we denote  $\tilde{p} = -p/\rho - gz$ . Now (1) and (2) are

$$\begin{aligned} \psi &= \tilde{p}, \\ \frac{\partial \mathbf{u}}{\partial t} + \mathbf{u} \cdot \nabla \mathbf{u} &= \nabla \tilde{p} + \nu \nabla^2 \mathbf{u}. \end{aligned} \quad (6)$$

**Two comments.** There are two discrepancies in what we model in the two domains: One is that the inviscid method may not handle vorticity. From our experience so far, it seems that we may handle this in practice by having the Navier-Stokes domain large enough so that vorticity of significance is not advected into the inviscid domain. The cpu time is not sensitive to the size of the CFD domain. The second discrepancy is that the linearized potential theory does not take into account nonlinearities, while the Navier-Stokes solver does via the term  $\mathbf{u} \cdot \nabla \mathbf{u}$ . If the free-surface flow becomes “non-linear”, the two solvers do not really solve for the same physics, and we expect problems. One example is in a closed sloshing tank, where nonlinearities become important quickly. Another example is in steep waves. A third example is shallow water waves. However, in gap resonance problems with small amplitude waves, the flow is well described by linear theory, and so the two different solvers solve the same physics, and the present domain-decomposition method becomes useful.

## Numerical implementation

In the potential domain we use a standard fourth order explicit Runge-Kutta (RK4) method to time-step the solution  $\varphi$  and  $\psi$  according to (5). Since both domains are solved simultaneously, we also use RK4 in the CFD domain. We use the standard way to solve the Navier-Stokes equations (2) and (4) numerically. This is done in three steps, referred to as the fractional step method. In principle, going from time-step  $n$  to  $n + 1$ : (A) advect  $u$  and  $w$ , (B) apply viscosity, and (C) solve Poisson equation and update to a divergence free velocity field  $\mathbf{u}^{n+1}$ . Steps (A) and (B) may be done in one single step, depending on what methods one choose for advection and diffusion. One may

say that the essential roles are for step (B) to create vorticity along walls, and for step (A) to advect this vorticity into the main part of the fluid. This creates circulation in the gap which acts like a damping. Step (C) is mathematically stated as

$$\nabla^2 \tilde{p} = \nabla \cdot \mathbf{u}^{**} / \Delta t, \quad \mathbf{u}^{n+1} = \mathbf{u}^{**} + \Delta t \tilde{p}, \quad (7)$$

where  $\mathbf{u}^{**}$  is the velocity field after steps (A) and (B), which is not divergence free, whereas  $\mathbf{u}^{n+1}$  is divergence free.

If we now look at the first equation in (6) we see that we may treat  $\tilde{p}$  and  $\psi$  as the same variable. Next compare the first equation in (5), and equation (7) and note that  $\tilde{p}$  and  $\psi$  are acted upon by the same operator; the Laplacian  $\nabla^2$ . If we choose the same numerical method to solve for  $\tilde{p}$  and  $\psi$ , we may use the same discretization method for both and we obtain one single system of equations  $Ax = b$  for the whole wavetank. This ensures that both matching conditions are satisfied without any further exchange of information between the two domains. In this way we avoid having an overlapping region, and we avoid any back-and-forth communication. There is a sharp interface between the two domains. To the authors’ knowledge, this method to couple potential theory with a Navier-Stokes solver has not been used earlier.

Since the domain  $\Omega_0$  is not changing, the system matrix  $A$  is constructed once and for all before the time stepping, and in the present implementation inverted using the Lapack banded solver. In this way, only a matrix-vector product is carried out each time-step.

We chose to use the Finite Volume Method in both domains. We discretize the whole wavetank by rectangles and assume all variables to be constant over each rectangle face. The method for advection is simply upwinding. This is diffusive, but sufficient for our purpose, where the shed vorticity is important only for about half a wave period. We call our code the *dd-code* hereafter.

## Results

Figure 2 (a - c) presents validation results for the present dd-code.  $A_g$  is the steady-state amplitude

averaged over the gap and  $A_f$  is the far-field amplitude. In all three cases (a - c) the main dimensions of the boxes are the same;  $B = 0.36\text{m}$ ,  $D/B = 0.5$ ,  $b/B = 0.25$ , the forced heave amplitude is  $\eta_{3a} = 5\text{mm}$ , and the water depth is  $h = 1.03\text{m}$ . What is varied is the appendage size  $s$  and  $d$ . The results called ‘‘Linear simulations’’ are also performed with the present dd-code with advection and diffusion turned off. This recovers the linear solution.

We see that linear theory overpredicts, as expected, while the simulations including flow separation (called ‘‘Present dd-code’’) compare well with the model tests. This indicates that the present dd-code is appropriate to use in analyzing gap resonance problems.

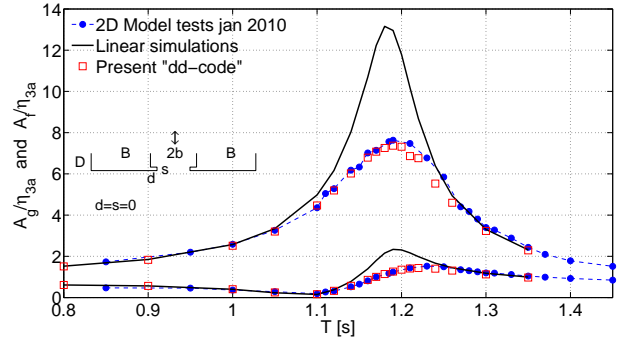
Steady-state was typically achieved after about 15 - 20 periods. Each marker in the figures is the average of the amplitude over the last 10 periods in a 30 period long run. The grid is near uniform around the body as shown in Figure 3 and stretched both in the vertical and horizontal directions away from the ship. We tried different resolutions: 4, 6, 10 and 20 grid cells across the gap. All gave practically the same results. This means the gap resonance problem is not sensitive to gridding.

The shown results are from the runs with 10 grid cells across the gap. For the whole wavetank we had  $n_x = 150$  and  $n_y = 54$ . The number of time-steps per period was 80. The cpu-time was remarkably low; running 30 periods (2400 time-steps) took only 73 seconds on a single 2.4GHz cpu. The simulations with flow separation took 20% more cpu-time than the linear simulations, basically due to the calculation of  $\nabla \cdot \mathbf{u}^{**}$  on the right hand side of the Poisson equation (7).

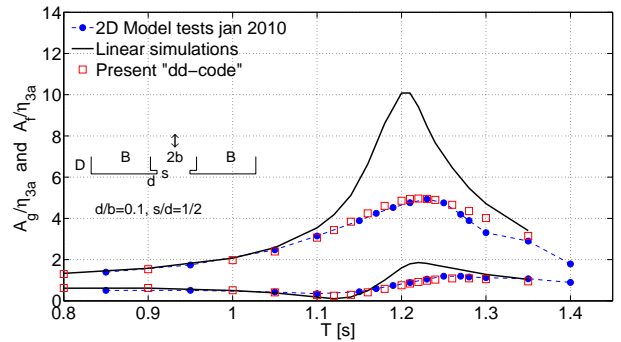
We mention that the same set-up as that presented in Figure 2 (a) was investigated in Kristiansen and Faltinsen (2008). They used a different set of model tests and different numerical models, but the results were almost identical.

## Ongoing and further work

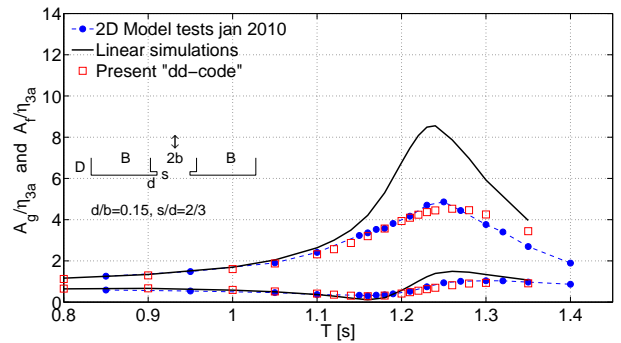
The results presented here is from a first version of the code which has a simple, body-fitted grid. Since the grid is rectangular, we may only model rectangular



(a) No appendages (square boxes)



(b) Small appendages



(c) Large appendages

Figure 2: Forced heave of two boxes.

shaped bodies. This is not adequate for an engineering tool. We are presently implementing an immersed boundary, so that the body may have arbitrary shape, while the grid is still rectangular. Next, we will implement local refinements by dividing some grid cells

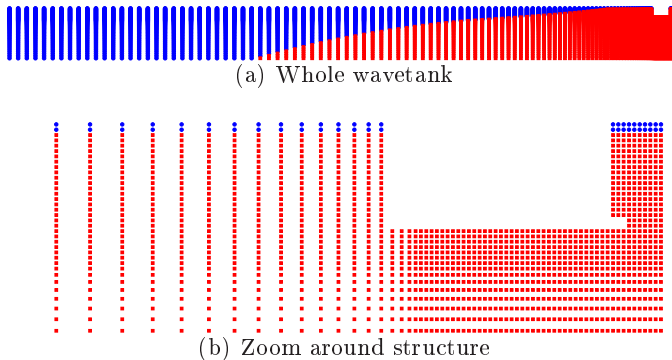


Figure 3: Blue: Potential domain. Red: CFD domain.

in four, and some of these in four again etc, so that details like bilge keels may be resolved.

Further, we are planning to add weakly nonlinear free surface conditions in particular in order to incorporate slowly varying motions which may bring the system out of resonance. Also we plan to include a current  $U$  in order to study wave-current-structure interaction including flow separation.

An engineering tool must be three-dimensional. The method is directly applicable in a three-dimensional setting. With an iterative solver that is parallelized, we expect that one may run three-dimensional simulations within minutes, and not days or weeks like traditional CFD codes.

### Concluding remarks

We have presented a new domain-decomposition strategy which couples linear potential theory with a Navier-Stokes solver (CFD) in a time-domain numerical wavetank. The intention was to provide a methodology for an engineer to analyze gap resonance problems in an efficient manner which is based on physics. The present implementation of the dd-code was validated against experiments, and the results were promising.

The major attractive feature about the method is that *one does not have CFD in the free surface zone*. The CFD domain is submerged in the fluid. This allows for a strong and sharp coupling between the two

domains. More importantly: Linearized potential theory is more accurate in propagating small-amplitude waves, and significantly faster. This means we gain both accuracy and cpu time.

The presented method is in principle directly applicable for a three-dimensional implementation.

### Acknowledgements

We gratefully acknowledge MARINTEK for allowing the use of the moonpool model test data.

### References

- Bunnik, T., W. Pauw, and A. Voogt (2009). Hydrodynamic analysis for side-by-side offloading. In *Proc. 19th Int. Offshore and Polar Eng. Conf.*
- Kristiansen, T. and O. M. Faltinsen (2008). Application of a vortex tracking method to the piston-like behaviour in a semi-entrained vertical gap. *Appl. Ocean Res.* 30, 1–16.
- Kristiansen, T. and O. M. Faltinsen (2009). A two-dimensional numerical and experimental study of resonant coupled ship and piston-mode motion. *Appl. Ocean Res.* 32, 158–176.
- Lu, L., L. C., B. T., and L. S. (2010). Comparison of potential flow and viscous fluid models in gap resonance. In *25th Int. Workshop on Water Waves and Floating Bodies*.
- McIver, P. (2005). Complex resonances in the water-wave problem for a floating structure. *J. Fluid Mech.* 536, 423–443.
- Molin, B., F. Remy, A. Camhi, and A. Ledoux (2009). Experimental and numerical study of the gap resonances in-between two rectangular barges. In *13th Congr. of Intl. Maritime Ass. of Mediterranean (IMAM)*.